PORTLAND PRESS

Research Article

A dual immune signature of CD8+ T cells and MMP9 improves the survival of patients with hepatocellular carcinoma

Huan Ding[1], Huan Hu[1], Feifei Tian[1] and Huaping Liang[2]

[1]School of Life Science and Engineering, Southwest Jiaotong University, Chengdu 610031, China; [2]State Key Laboratory of Trauma, Burns and Combined Injury, Department of Wound Infection and Drug, Daping Hospital, Army Medical University, Chongqing 400010, China

Correspondence: Feifei Tian (tulwar@home.swjtu.edu.cn) or Huaping Liang (13638356728@163.com)

OPEN ACCESS

The 5-year survival of hepatocellular carcinoma (HCC) is difficult due to the high recurrence rate and metastasis. Tumor infiltrating immune cells (TICs) and immune-related genes (IRGs) bring hope to improve survival and treatment of HCC patients. However, there are problems in predicting immune signatures and identifying novel therapeutic targets. In the study, the CIBERSORT algorithm was used to evaluate 22 immune cell infiltration patterns in gene expression omnibus (GEO) and the cancer genome atlas (TCGA) data. Eight immune cells were found to have significant infiltration differences between the tumor and normal groups. The CD8+ T cells immune signature was constructed by least absolute shrinkage and selection operator (LASSO) algorithm. The high infiltration level of CD8+ T cells could significantly improve survival of patients. The weighted gene co-expression network analysis (WGCNA) algorithm identified MMP9 was closely related to the overall survival of HCC patients. K-M survival and tROC analysis confirmed that MMP9 had an excellent prognostic prediction. Cox regression showed that a dual immune signature of CD8+ T cells and MMP9 was independent survival factor in HCC. Therefore, a dual prognostic immune signature could improve the survival of patient and may provide a new strategy for the immunotherapy of HCC.

Introduction

Hepatocellular carcinoma is one of the common fatal malignant tumors in clinical [1]. It mainly developed from hepatitis and cirrhosis [2]. The early symptoms of HCC are relatively insidious, and most patients are already at an advanced stage when they are diagnosed [3]. Recently, new treatment methods have made some progress in the treatment of liver cancer [4]. However, the patient's prognosis is still not satisfactory due to the high recurrence and metastasis of HCC [5]. Therefore, the determination of reliable prognostic markers is the key to improving the prognosis of HCC patients.

The tumor immune microenvironment is the environment where tumors interact with the immune system. The development of tumor was accompanied by mutual restriction between tumor and immune cells [6]. On the one hand, the immune system plays an antitumor effect by recognizing and killing tumor cells. On the other hand, tumor cells mainly promote tumorigenesis by immune suppression and immune tolerance [7]. With the rise of immunotherapy, immune checkpoint inhibitors (PD-1, CART, CTLA4, PD-L1 and PD-Ls) have made progress in the treatment and prognosis of HCC patients [8,9]. However, the disadvantage is that the treatment strategy is only applicable to a small number of patients. And there are problems in predicting immune signatures and identifying novel therapeutic targets. Studies revealed that the infiltration of TICs (tumor infiltrating immune cells) in malignant tumor cells is closely related to the expression of PD-1/PD-L1 [10,11]. The function and composition of TICs changed with the host immune status. Studies have reported the prognostic value of TICs in lung cancer, breast cancer and squamous cell

carcinoma [12–14]. Accordingly, an extensive study of the immune infiltration pattern of TICs would help elucidate complex antitumor responses to improve the survival of HCC.

CIBERSORT [15] is a deconvolution algorithm based on a set of barcode gene expression, which is superior to other methods in the identification and of immune cells. The method can accurately quantify the level of infiltration of specific cell types. Moreover, the ESTIMATE can evaluate the tumor microenvironment's matrix abundance and tumor purity [16].

Our previous research has identified various biomarkers and potential inflammation-modulating therapeutic targets through experimental and bioinformatics method [17–19]. In the study, CIBERSORT was used to calculate the proportion of immune cells in GEO and TCGA database. A dual prognostic immune signature of TIC and IRG was constructed based on LASSO and WGCNA algorithms. Univariate and multivariate COX confirmed the potential value of the dual signature for improving the survival prediction of HCC.

Materials and methods

Collection and extraction of data

GSE76427 that contained 115 HCC samples and 52 normal samples came from GEO (https://www.ncbi.nlm.nih.gov/geo). The mRNA-seq (tumor = 371, normal = 50) expression data and corresponding clinical information were download in the TCGA database (https://cancergenome.nih.gov/; July 2020). The expression data was processed by log2 conversion. Samples with survival time < 1 day were excluded. The 2483 immune-related genes (Supplementary File S1) had been identified according to the ImmPort database (https://immport.niaid.nih.gov; July 2020). The overlapping IRGs were selected between the TCGA, GEO and ImmPort dataset.

Analysis of immune fluctuation in HCC microenvironment

The CIBERSORT algorithm was used to calculate the proportion of 22 immune cells in each patient (perm = 1000). And the difference of immune cell infiltration were evaluated in tumor and normal tissues. The ESTIMATE algorithm was used to calculate the immune scores and matrix score of all samples. TIMER (https://cistrome.shinyapps.io/timer/) is used to analyze the correlation between prognostic IRG signature and immune cell infiltration.

Construction of immune cell signature

The patient's OS status and time was obtained from GEO and TCGA cohort. Univariate COX regression initially screened immune cells related to the patient's life cycle ($P<0.05$). The LASSO model used a punishment mechanism to screen out prognostic signatures associated with the survival of the patient. The overlapping TICs signatures were selected between GEO and TCGA cohort. LASSO could be expressed as a constraint on the objective function.

$$\min_{\omega} \sum_{j=1}^{m} \left(y_j - \sum_{i=1}^{n} \chi_{ji}\omega_i \right)^2, s.t. \sum_{i=1}^{n} |\omega_i| \leqslant \lambda$$

WGCNA analysis

The expression matrix was established based on the overlapping IRGs of GEO data. The R package 'WGCNA v1.69' was used to build a co-expression network. The modules with potent immune characteristics were determined by calculating the correlation between each module and immune characteristics ($P<0.05$). The algorithm steps were as follows:
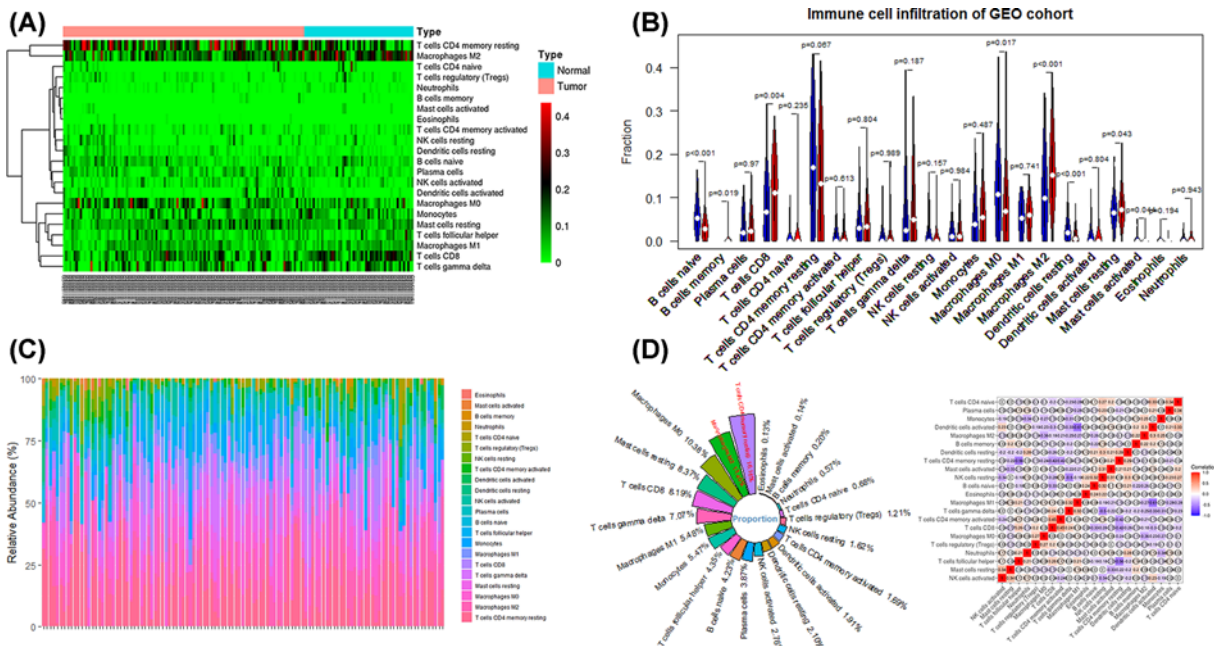
The Pearson algorithm was used to calculate the similarity between two genes, and then construct a correlation matrix.

$$Y = |S_{ij}| = \left| \frac{1 + \text{cor}(x_i + y_i)}{2} \right|$$

A topological overlap matrix was created by calculating the adjacency matrix.

$$A = a_{ij} = \text{power}(S_{ij}, \beta) = S_{ij}^{\beta}$$

$$\text{TOM} = \frac{\Sigma_{k \neq ij} A_{ik \cdot A_{kj}} + A_{ij}}{\min(\Sigma_k A_{ik} + \Sigma_k A_{jk}) + 1 - A_{ij}}$$

Figure 1. Analysis of 22 immune cell infiltration according to CIBERSORT algorithm
(**A**) Heatmap of 22 immune cells. (**B**) Differences of 22 immune cells infiltration between the HCC and Normal group. (**C**) The percentage of immune cells in HCC sample. (**D**) Average infiltration rate and correlation analysis.

The module membership was built.

$$ME = \mathrm{princomp}\left(X_{ij}^{q}\right)$$

$$MM_{i}^{q} = \mathrm{cor}\left(X_{i}, ME^{q}\right)$$

Evaluation of prognostic value

The prognostic performance of immune signature was evaluated by Kaplan–Meier survival and tROC curve. The 'Correlation Analysis' module of GEPIA2 was used to evaluate the correlation between IRG signature and immune cell marker genes. Univariate and multivariate Cox regression were used to analyze the immune characteristics and clinical parameters.

Statistical

Bioinformatics analysis was executed by using R v3.6.1 and its corresponding packages. $P<0.05$ was considered statistically significant.

Results

Immune cell infiltration pattern of HCC

The CIBERSORT algorithm described the infiltration pattern of 22 immune cells in the GEO cohort and TCGA cohort. The immune score of each sample was calculated according to the ESTIMATE algorithm (Supplementary File S2). Heat map of the distribution of 22 immune cells in the GEO cohort (Figure 1A). B cells naive ($P<0.001$), B cells memory ($P=0.019$), T cells CD8 ($P=0.004$), Macrophages M0 ($P=0.017$), Macrophages M2 ($P<0.001$), Dendritic cells resting ($P<0.001$), Mast cells resting ($P=0.043$), Mast cells activated ($P=0.044$), there were significant infiltration differences between HCC and normal tissues (Figure 1B). The percentage of immune cells in each HCC sample was shown in Figure 1C. And the average infiltration rate of immune cells and the correlation matrix were shown in Figure 1D.
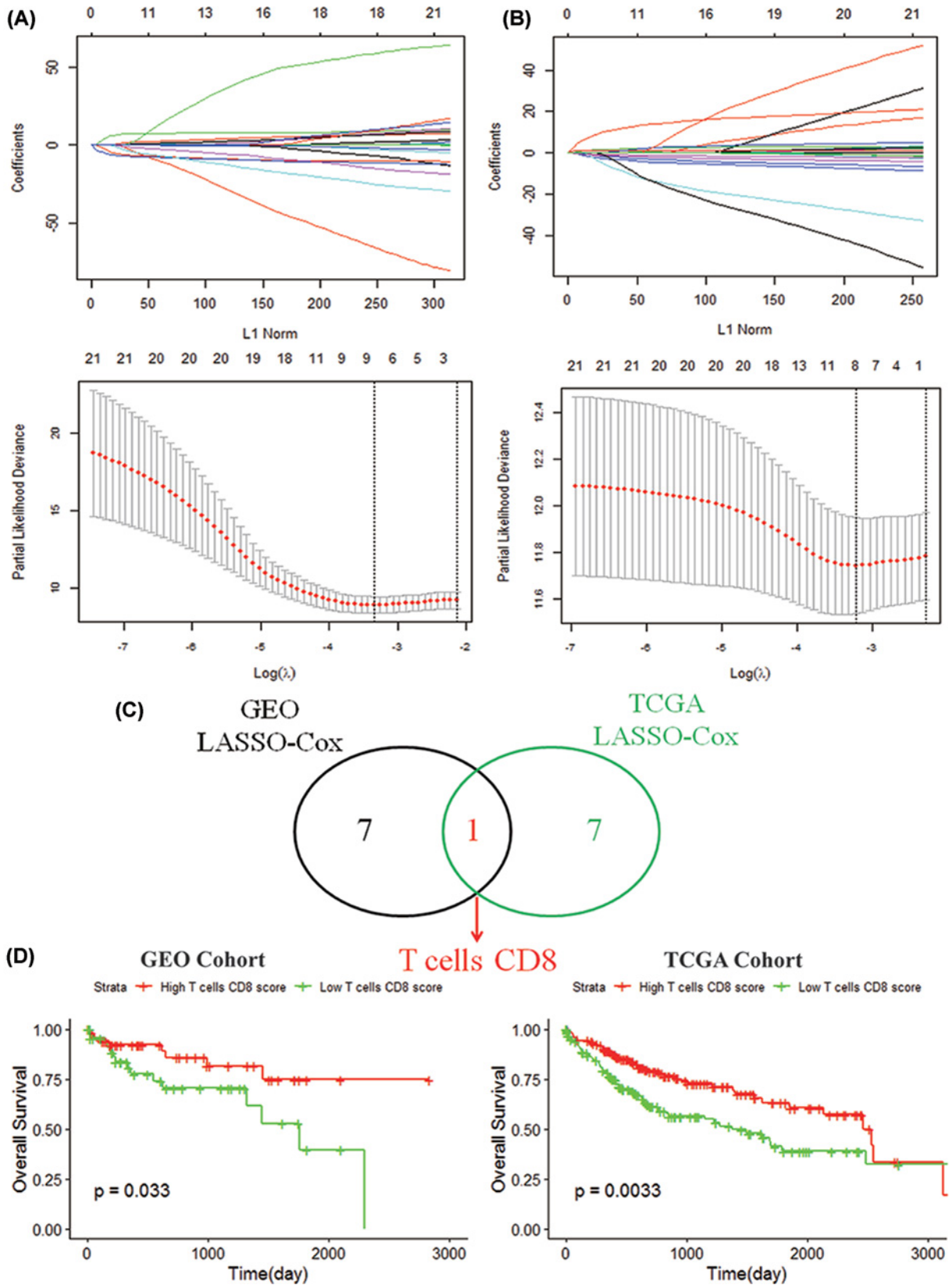
Figure 2. Definition and prognostic analysis of CD8+ T Cells

(**A**) LASSO analysis identified eight TICs in GEO cohort. (**B**) Determine the minimum value of λ to be eight based on TCGA cohort. (**C**) Identification of CD8+ T cells. (**D**) Survival analysis of CD8+ T cells.
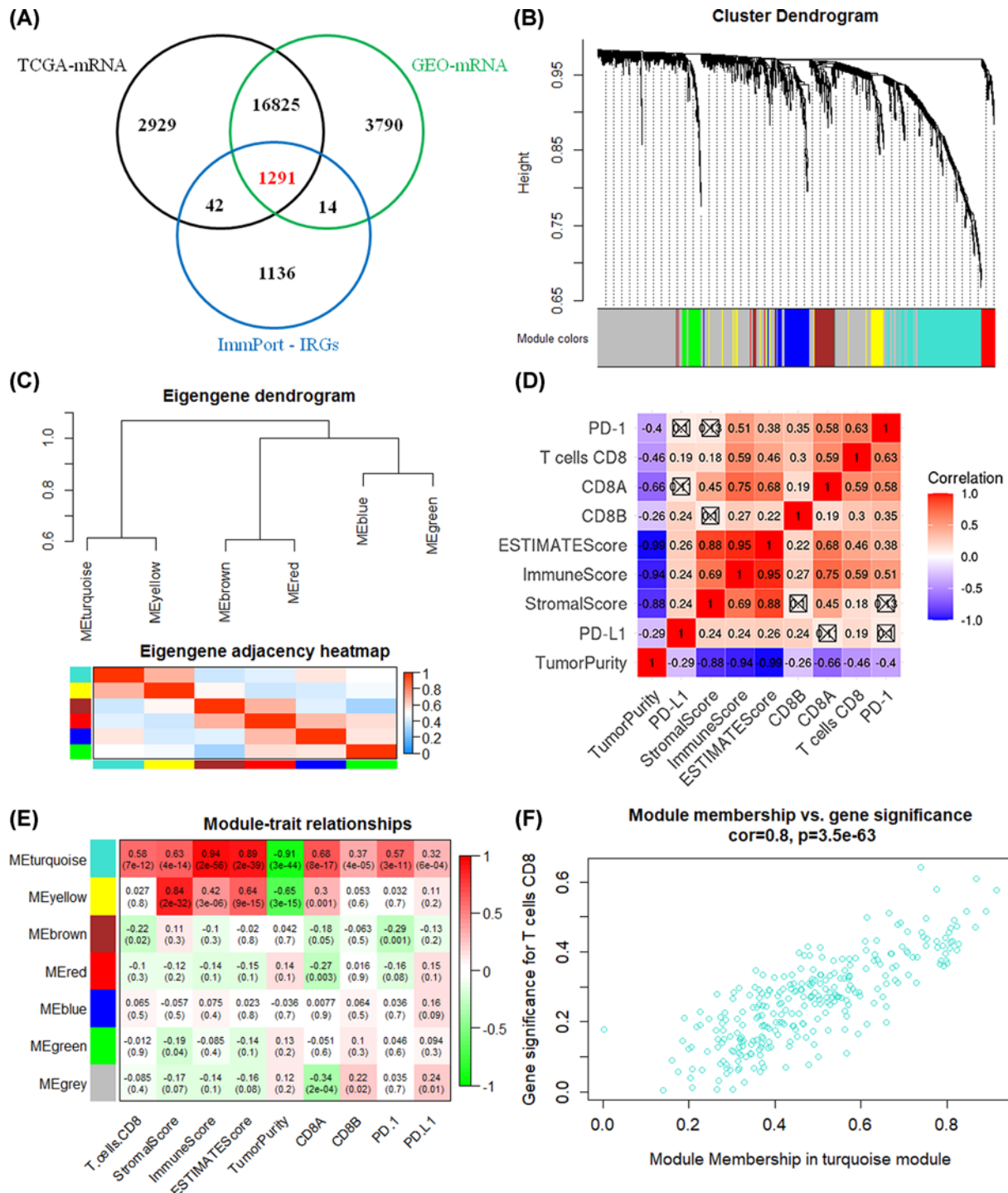
Figure 3. Identification of key IRGs based on WGCNA

(**A**) 1291 overlapping IRGs from three databases. (**B**) A dendrogram of IRGs including gray modules (genes not classified into modules). (**C**) Module–module correlation analysis diagram. (**D**) Correlation analysis between CD8+ T cells and eight immune characteristics. (**E**) Correlation heatmap of modules and immune traits. The turquoise module showed outstanding correlation. (**F**) In-depth analysis of the correlation between turquoise module and T cell CD8.
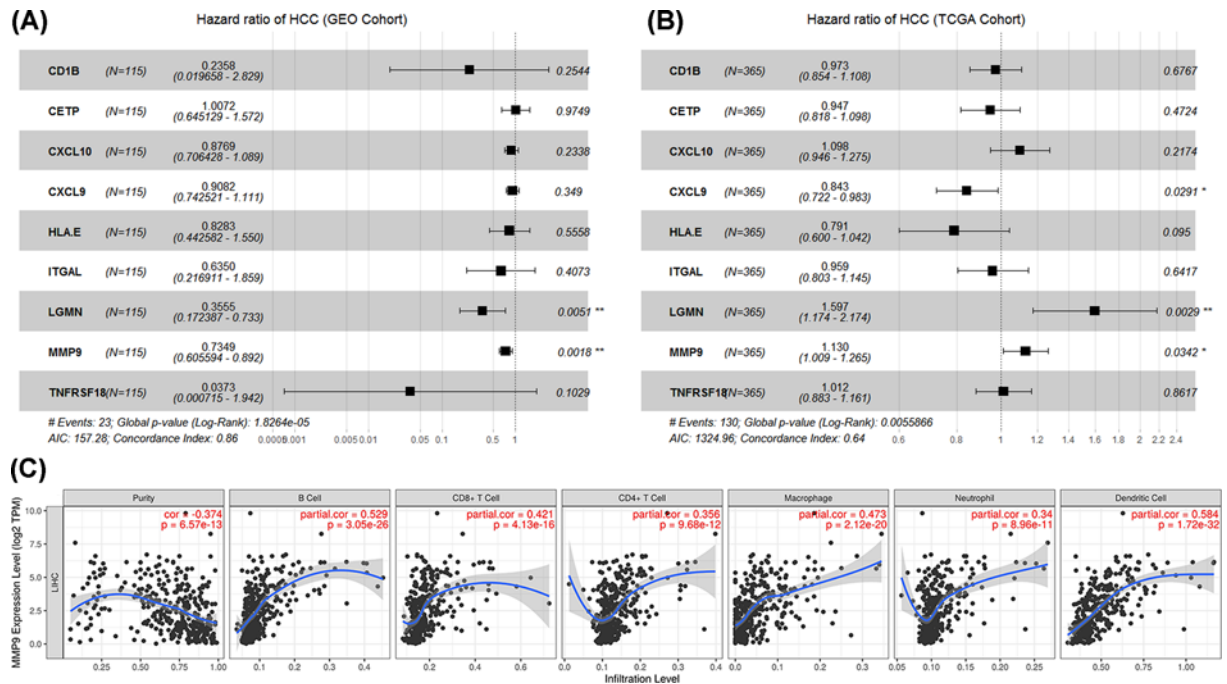
Figure 4. Construction of MMP9 signature
(**A** and **B**) Multivariate COX regression of nine IRGs in GEO cohort and TCGA cohort. (**C**) Correlation analysis between the expression of MMP9 and immune cells based on TIMER.

Determination and prognostic significance of TIC signature

The eight TICs immune signatures were obtained based on univariate COX regression and LASSO analysis (Figure 2A,B). CD8+ T cells was identified by Venn analysis (Figure 2C). The survival curve showed that the high infiltration level of CD8+ T cells could significantly improve survival of HCC (Figure 2D).

Identification of IRG modules related to TIC signature

The expression data of 1291 overlapping IRGs were screened to perform WGCNA analysis (Figure 3A). The six modules were identified by constructing a scale-free network (Figure 3B). The module correlation analysis demonstrated that turquoise strongly correlated with the yellow module (Figure 3C). CD8+ T cells was significantly correlated with eight immunophenotypic parameters (PD-1, PD-L1, CD8A, CD8B, ImmuneScore, ImmuneScore, ESTIMATEScore, TumorPurity) (Figure 3D). The turquoise module had a strong correlation with nine immunophenotypic parameters (Figure 3E). Further analysis indicated that the turquoise module were significantly correlated with CD8+ T cells (cor = 0.80, $P = 3.5e-63$) (Figure 3F). Therefore, the turquoise module (278 IRGs) was identified as a key module.

Construction and prognostic value of immune IRG signature

The 36 IRGs were identified to be significantly related to the patient's OS in the GEO cohort ($P<0.05$) through univariate COX regression analysis. Nine IRGs signatures were obtained by LASSO COX analysis (Supplementary Figure S1). MMP9 was identified as a prognostic immune signature based on GEPIA2 correlation analysis (Table 1 and Supplementary Table S1) and multivariate COX regression analysis (Figure 4A,B). TIMER evidenced that the high expression of MMP9 significantly increased the infiltration level of the B cells (cor = 0.529, $P = 3.05e-26$), CD8+ T cells (cor = 0.421, $P = 4.13e-16$), CD4+ T cells (cor = 0.356, $P = 9.68e-12$), macrophage (cor = 0.473, $P = 2.12e-20$), neutrophil (cor = 0.34, $P = 8.96e-11$), dendritic cells (cor = 0.584, $P = 1.72e-32$). Interestingly, the increased expression of MMP9 could reduce tumor purity (Figure 4C).

The GEO cohort found that the expression of MMP9 was significantly up-regulated in tumor tissues ($P=0.00016$). The high expression of MMP9 corresponded to the poor survival of HCC ($P=0.0013$). The tROC curve analysis evidenced that the MMP9 signature had an excellent prognostic predictive effect (Figure 5A). The TCGA cohort analysis results also confirmed that MMP9 had significant prognostic value (Figure 5B).

Table 1 Correlation analysis between gene signature and CD8A, CD8B

| Gene	CD8A		CD8B	
	Cor	***P*.value**	**Cor**	***P*.value**
CD1B	0.24	3.2e−08	0.23	5.4e−08
CETP	0.16	2e−04	0.14	0.0011
CXCL10	0.45	0	0.41	0
CXCL9	0.72	0	0.64	0
HLA-E	0.48	0	0.45	0
ITGAL	0.49	0	0.43	0
LGMN	0.54	0	0.53	0
MMP9	0.18	4.6e−05	0.17	9.4e−05
TNFRSF18	0.22	2.8e−07	0.23	1.1e−07
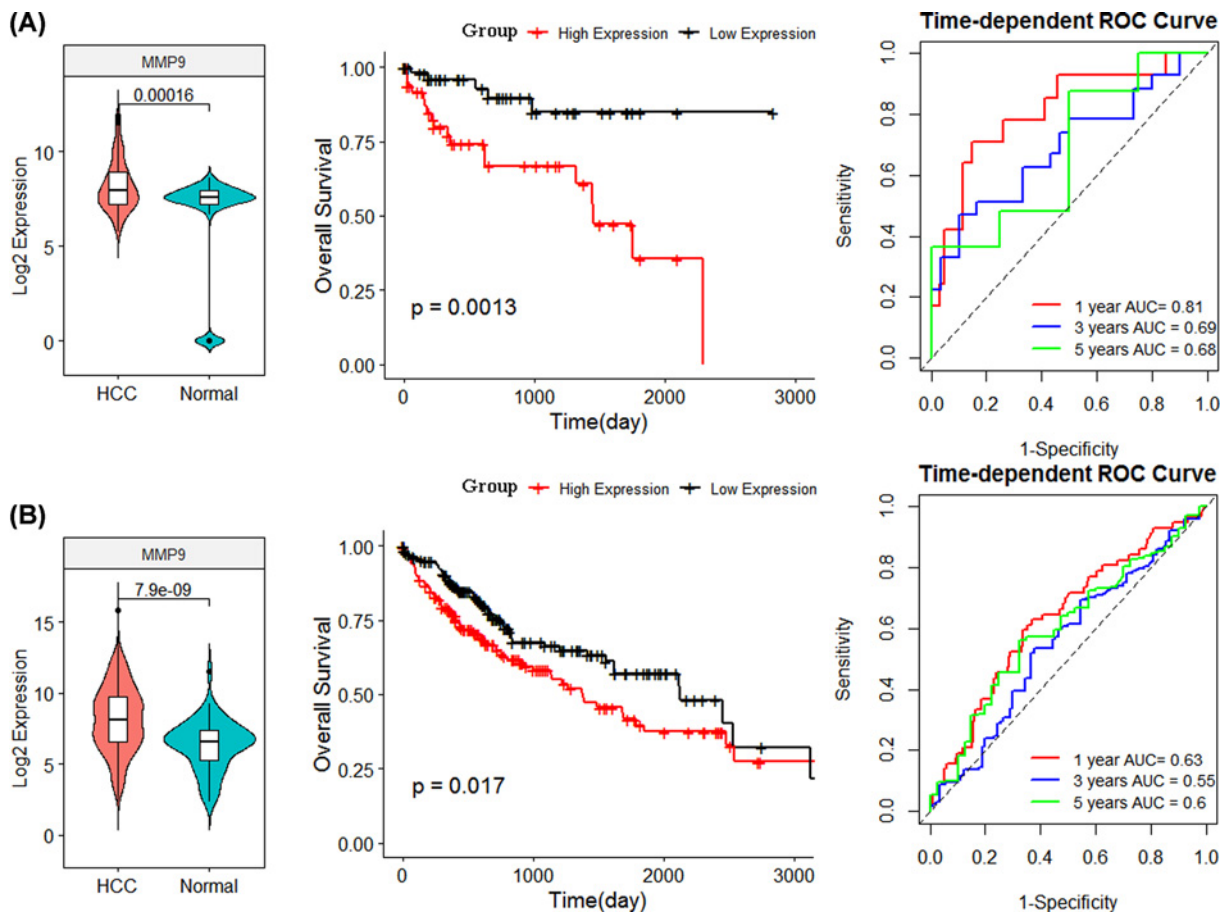
Figure 5. Prognostic value of MMP9
(**A** and **B**) Analysis of expression patterns, survival and tROC based on GEO cohort and TCGA cohort.

We characterized the mutants of the TCGA cohort based on the expression of MMP9. The 20 genes were observed with the highest mutation frequency in the TCGA cohort. We found that basically all genes had higher mutation frequency in the high expression group than in the low expression group (Figure 6). All samples were dominated by mutations of TTN, TP53 and MUC16.

The immune infiltration landscape of MMP9 in HCC

To further confirm the immunity of MMP9, we evaluated the immune infiltration landscape of different expression groups based on TCGA data. We found that T cells CD4 memory resting (high = 23.41%, low = 22.23%),
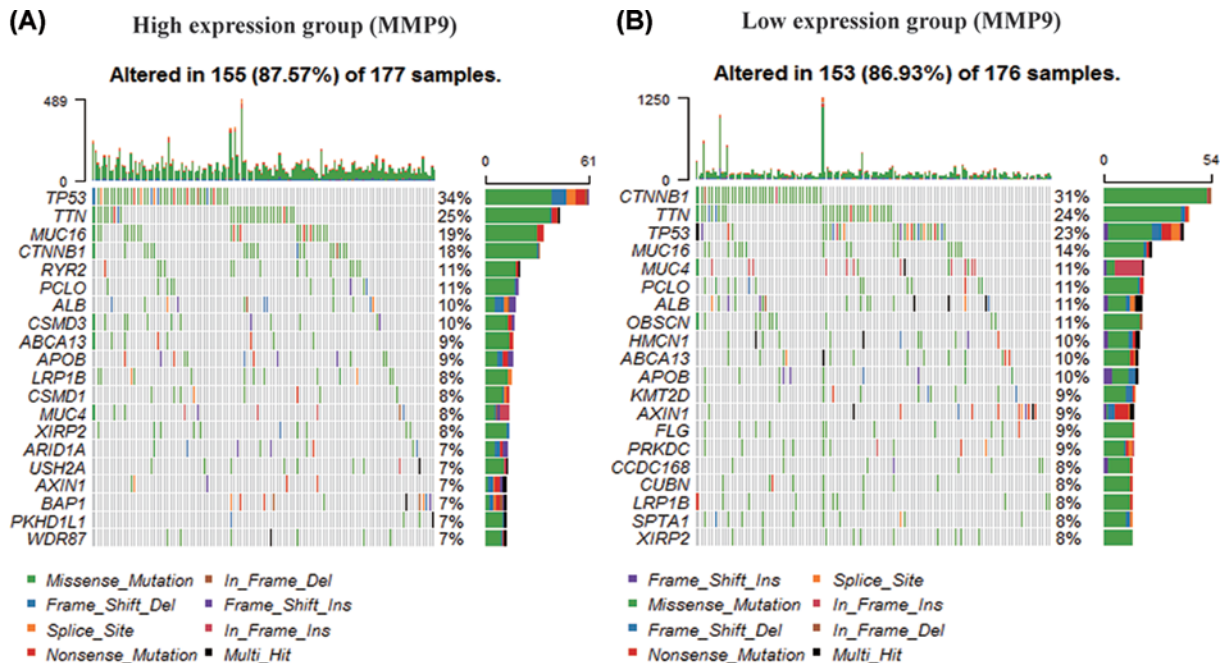
Figure 6. Correlation analysis between the MMP9 and HCC mutations from TCGA cohort
(**A** and **B**) The mutation status of the top 20 genes in the high and low expression group.

Macrophages M2 (high = 17.95%, low = 18.10%) and Macrophages M0 (high = 12.28%, low = 12.02%) were among the infiltration ratios more than 50% (Figure 7A,B). Compared with the low expression group, B cells naïve ($P=0.032$), B cells memory ($P=0.006$), T cells CD8 ($P=0.002$), T cells CD4 naïve ($P<0.001$), T cells CD4 memory resting ($P=0.036$), T cells CD4 memory activated ($P<0.001$), T cells follicular helper ($P=0.029$), T cells regulatory (Tregs) ($P<0.001$), NK cells activated ($P<0.001$), monocytes ($P<0.001$), macrophages M0 ($P<0.001$), dendritic cells resting ($P<0.001$), dendritic cells activated ($P=0.03$) and mast cells resting ($P<0.001$) had significant differences (Figure 7C).

## Independent prognostic analysis of TIC signature and IRG signature

The univariate COX regression model of GEO cohort indicated that a dual signature of CD8+ T cells (HR = 0.020, $P=0.017$) and MMP9 (HR = 0.772, $P<0.001$) was significantly related to the survival of HCC patients. Multivariate COX revealed that a dual signature of CD8+ T cells (HR = 0.000247, $P=0.0198$) and MMP9 (HR = 0.783443, $P=0.0021$) was an independent predictor of the prognosis of HCC (Figure 8A). Similarly, TCGA cohort analysis also confirmed this result (Figure 8B).

Discussion

Tumor microenvironment played a critical role in the tumor progression. Abundant evidence shows that TICs play an essential role in predicting tumor progression and prognosis [20]. The distribution of TICs is significantly different between different tumor stages or different types of tumors. The evaluation of the number, phenotype and spatial distribution of TICs may provide reliable treatment strategies of patients. At present, most studies have focused on RNA signatures to predict prognosis and the role of TICs in the progression and treatment of HCC [21–25]. However, the predictive capability of single biomarker is usually defective. Conversely, the combination of immunotherapy and targeted therapy is expected to improve the survival after standard treatment in cancer. But the value of the dual signature combining TIC and IRG in improving the survival of HCC has not been studied yet. Therefore, in the preent study, a dual immune prognostic model was constructed through GEO, TCGA and ImmPort dataset, which may provide a new strategy for improving the survival and immunotherapy of HCC.

This study described the distribution of TICs in HCC based on CIBERSORT. LASSO analysis confirmed that only CD8+ T cells was significantly correlated with the overall survival of HCC. We found that the infiltration pattern of CD8+ T cells was significantly different between HCC and normal groups. High infiltration levels of CD8+ T
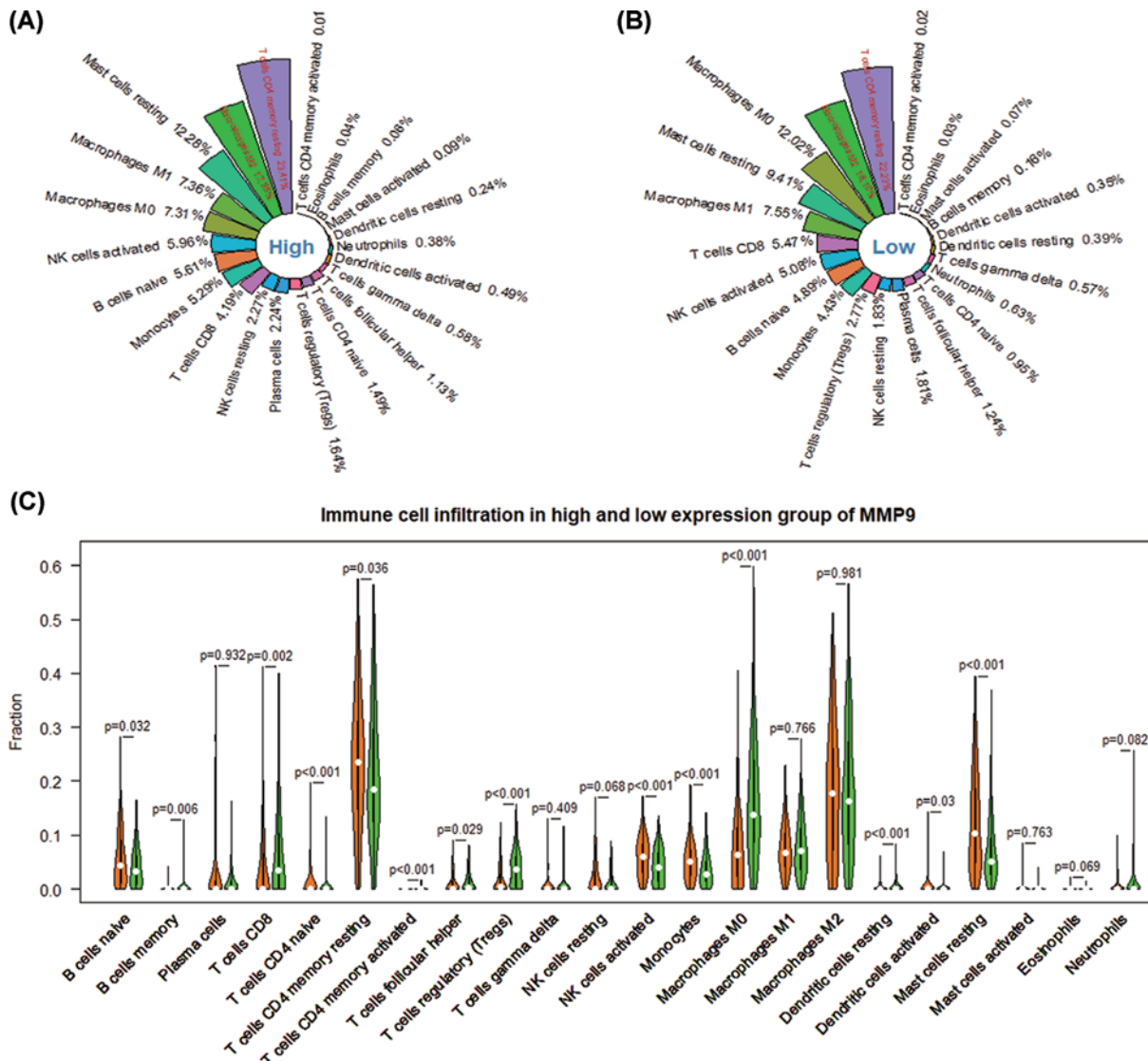
Figure 7. Immune infiltration levels in high and low expression groups of MMP9
(**A** and **B**) The infiltration proportion of 22 immune cells in the high and low expression groups. (**C**) Differences in the level of immune cell infiltration between the high and low expression groups.

cells could improve the prognosis of HCC. Besides, we studied the complicated relationship between T-cell CD8 and routine clinical parameters to reveal whether T cell CD8 is an independent variable of HCC. Interestingly, Cox regression analysis confirmed that CD8+ T cell is an independent prognostic factor of HCC. Sometimes CD8+ T cells killed cancer cells, but they promoted cancer cell proliferation occasionally. Most CD8+ T cells are activated and transformed into cytotoxic T lymphocytes to play a direct killing effect by recognizing TAA [26]. However, CD8+ T cells promotes the proliferation of HCC by maintaining immune tolerance [27]. Huang et al. reported that the expression of PD-L1 is significantly related to CD8+ T cells in HCC [28]. Guo et al. found that the expression of CD8 + T cells in HCC was significantly higher than in normal tissues [29]. CD8+ T cells is related to the progression and prognosis of HBV-HCC [30]. These studies indicate that T cell CD8 plays an essential role in the process of HCC. And it is a specific marker for evaluating the prognosis of HCC.

Cytotoxic T lymphocytes (CTL) in the HCC microenvironment are mainly CD8+ T cells [31]. Interferon (IFN)-γ produced by CD8+ T cells is a key factor in antitumor immunity. It can increase antigen presentation, proinflammatory cytokine production and directly kill tumor cells [32]. Preclinical studies have found that exposure of tumors to IFN-γ secreted by antigen-specific CD8+ T cells can lead to tumor cells' genetic instability. DNA damage
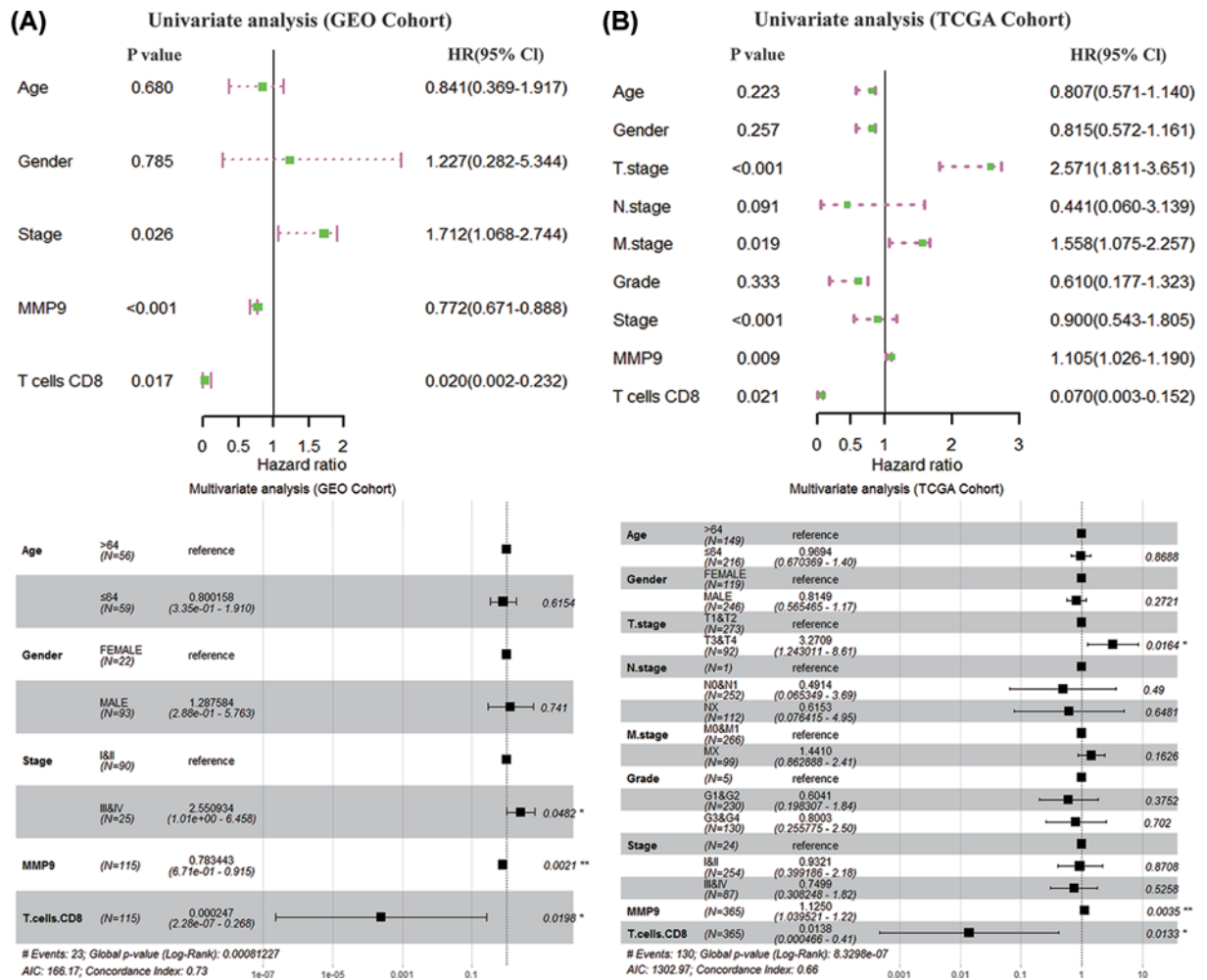
Figure 8. Independent prognostic analysis

(**A** and **B**) Univariate and multivariate COX analysis based on GEO cohort and TCGA cohort.

response-related copy number variation, DNA editing, and DNA repair-related gene changes [33]. CD8+CXCR5+T in HCC produces IL-21 (interleukin-21), which induces B cells to differentiate into plasma cells that produce Ig G. And it plays a key role in the humoral immunity of HCC, which is related to a good prognosis [34]. HIF-α1 induced the increase of TREM-1 expression in TAMs, impairing the cytotoxic function of CD8+T cells and inducing apoptosis. And it blocks spontaneous and PD-L1 antibody-mediated anti-HCC effects [35]. The depleted CD8+ T cells seem to have evolved in the liver, and immunotherapy may restore the depleted T cells in the HCC [36]. Therefore, CD8 + T cells play an important role in the progression of HCC.

MMP9 is a member of the zinc-dependent endoprotease family. It is involved in processes such as inflammation, apoptosis and immunity [37]. Wang et al. found that high expression of MMP9 was significantly associated with HCC metastasis [38]. And The MMP9 expression was significantly correlated with the penetration level of TICs. Liu et al. confirmed that macrophages M2 affects the progression of HCC through MMP9 [39]. MMP9 acted actively to regulate the immune response and pathogenesis of HCC [40,41]. In our study, the survival curve, tROC curve and COX regression analysis confirmed that MMP9 was an independent indicator predicting the survival of HCC.

In conclusion, our study confirmed that a dual immune signature of CD8+ T cells and MMP9 could improve the survival of HCC. But the application potential of a dual immune signature in HCC immunotherapy still needs sufficient experimental verification.

Data Availability

The datasets analyzed in this study are available in Gene Expression Omnibus (GEO) and The Cancer Genome Atlas (TCGA).

PORTLAND
PRESS

Competing Interests
The authors declare that there are no competing interests associated with the manuscript.

Funding

Author Contribution
H.D.: Methodology, reviewed relevant literature and wrote the manuscript. H.H.: Prepare some data. F.T.: Contributed to the discussion. H.L.: Supervised the whole project.

Abbreviations
GEO, gene expression omnibus; HCC, hepatocellular carcinoma; IRG, immune-related gene; K-M, Kaplan–Meier; LASSO, least absolute shrinkage and selection operator; OS, overall survival; TCGA, the cancer genome atlas; TIC, tumor infiltrating immune cell; WGCNA, weighted gene coexpression network analysis.

References

1 Armengol, C. et al. (2018) Hepatocellular carcinoma: present and future. *Med. Clin. (Barc)* **150**, 390–397, https://doi.org/10.1016/j.medcli.2017.08.010

2 Jindal, A. et al. (2019) Hepatocellular carcinoma: etiology and current and future drugs. *J. Clin. Exp. Hepatol.* **9**, 221–232, https://doi.org/10.1016/j.jceh.2019.01.004

3 Hartke, J. et al. (2017) The diagnosis and treatment of hepatocellular carcinoma. *Semin. Diagn. Pathol.* **34**, 153–159, https://doi.org/10.1053/j.semdp.2016.12.011

4 Kumari, R. et al. (2018) Hepatocellular carcinoma treatment: hurdles, advances and prospects. *Hepat. Oncol.* **5**, HEP08, https://doi.org/10.2217/hep-2018-0002

5 Sim, H.W. and Knox, J. (2018) Hepatocellular carcinoma in the era of immunotherapy. *Curr. Probl. Cancer* **42**, 40–48, https://doi.org/10.1016/j.currproblcancer.2017.10.007

6 Lei, X. et al. (2020) Immune cells within the tumor microenvironment: biological functions and roles in cancer immunotherapy. *Cancer Lett.* **470**, 126–133, https://doi.org/10.1016/j.canlet.2019.11.009

7 Liu, Y. and Cao, X. (2016) Immunosuppressive cells in tumor immune escape and metastasis. *J. Mol. Med. (Berl.)* **94**, 509–522, https://doi.org/10.1007/s00109-015-1376-x

8 Mocan, T. et al. (2019) Programmed cell death protein-1 (PD-1)/programmed death-ligand-1 (PD-L1) axis in hepatocellular carcinoma: prognostic and therapeutic perspectives. *Clin. Transl. Oncol.* **21**, 702–712, https://doi.org/10.1007/s12094-018-1975-4

9 Agdashian, D. et al. (2019) The effect of anti-CTLA4 treatment on peripheral and intra-tumoral T cells in patients with hepatocellular carcinoma. *Cancer Immunol. Immunother.* **68**, 599–608, https://doi.org/10.1007/s00262-019-02299-8

10 Li, J. et al. (2018) Co-inhibitory molecule B7 superfamily member 1 expressed by tumor-infiltrating myeloid cells induces dysfunction of anti-tumor CD8(+) T cells. *Immunity* **48**, 773e5–786e5

11 Xie, M. et al. (2019) Prognostic and clinicopathological significance of PD-1/PD-L1 expression in the tumor microenvironment and neoplastic cells for lymphoma. *Int. Immunopharmacol.* **77**, 105999, https://doi.org/10.1016/j.intimp.2019.105999

12 Xu, F. et al. (2020) Immune signature of T follicular helper cells predicts clinical prognostic and therapeutic impact in lung squamous cell carcinoma. *Int. Immunopharmacol.* **81**, 105932, https://doi.org/10.1016/j.intimp.2019.105932

13 Gu-Trantien, C. et al. (2013) CD4(+) follicular helper T cell infiltration predicts breast cancer survival. *J. Clin. Invest.* **123**, 2873–2892, https://doi.org/10.1172/JCl67428

14 Che, Y. et al. (2020) Immune signature of tumor-infiltrating immune cells predicts the prognosis and therapeutic effects in squamous cell carcinoma. *Int. Immunopharmacol.* **87**, 106802, https://doi.org/10.1016/j.intimp.2020.106802

15 Newman, A.M. et al. (2015) Robust enumeration of cell subsets from tissue expression profiles. *Nat. Methods* **12**, 453–457, https://doi.org/10.1038/nmeth.3337

16 Yoshihara, K. et al. (2013) Inferring tumour purity and stromal and immune cell admixture from expression data. *Nat. Commun.* **4**, 2612, https://doi.org/10.1038/ncomms3612

17 Tian, F. et al. (2015) The small-molecule inhibitor selectivity between IKKalpha and IKKbeta kinases in NF-kappaB signaling pathway. *J. Recept. Signal Transduct. Res.* **35**, 307–318, https://doi.org/10.3109/10799893.2014.980950

18 Tian, L.X. et al. (2020) Knockout of cytochrome P450 1A1 enhances lipopolysaccharide-induced acute lung injury in mice by targeting NF-kappaB activation. *FEBS Open Bio.*, https://doi.org/10.1002/2211-5463.12977

19 Fan, X. et al. (2017) Evodiamine inhibits zymosan-induced inflammation in vitro and in vivo: inactivation of NF-kappaB by inhibiting IkappaBalpha phosphorylation. *Inflammation* **40**, 1012–1027, https://doi.org/10.1007/s10753-017-0546-0

20 Fridman, W.H. et al. (2012) The immune contexture in human tumours: impact on clinical outcome. *Nat. Rev. Cancer* **12**, 298–306, https://doi.org/10.1038/nrc3245

21 Zheng, Z. et al. (2020) Construction of a 13-microRNA-based signature and prognostic nomogram for predicting overall survival in patients with hepatocellular carcinoma. *Hepatol. Res.* **50**, 1151–1163, https://doi.org/10.1111/hepr.13538

22 Liu, G.M. et al. (2020) Identification of a four-gene metabolic signature predicting overall survival for hepatocellular carcinoma. *J. Cell. Physiol.* **235**, 1624–1636, https://doi.org/10.1002/jcp.29081

23 Gu, J.X. et al. (2019) Six-long non-coding RNA signature predicts recurrence-free survival in hepatocellular carcinoma. *World J. Gastroenterol.* **25**, 220–232, https://doi.org/10.3748/wjg.v25.i2.220

24 Garnelo, M. et al. (2017) Interaction between tumour-infiltrating B cells and T cells controls the progression of hepatocellular carcinoma. *Gut* **66**, 342–351, https://doi.org/10.1136/gutjnl-2015-310814

25 Zhou, G. et al. (2017) Antibodies against immune checkpoint molecules restore functions of tumor-infiltrating T cells in hepatocellular carcinomas. *Gastroenterology* **153**, 1107e10–1119e10, https://doi.org/10.1053/j.gastro.2017.06.017

26 Tauber, C. et al. (2019) Inefficient induction of circulating TAA-specific CD8+ T-cell responses in hepatocellular carcinoma. *Oncotarget* **10**, 5194–5206, https://doi.org/10.18632/oncotarget.27146

27 Langhans, B. et al. (2019) Role of regulatory T cells and checkpoint inhibition in hepatocellular carcinoma. *Cancer Immunol. Immunother.* **68**, 2055–2066, https://doi.org/10.1007/s00262-019-02427-4

28 Huang, C.Y. et al. (2017) Relationship between PD-L1 expression and CD8+ T-cell immune responses in hepatocellular carcinoma. *J. Immunother.* **40**, 323–333, https://doi.org/10.1097/CJI.0000000000000187

29 Guo, M. et al. (2020) Expression and clinical significance of LAG-3, FGL1, PD-L1 and CD8(+)T cells in hepatocellular carcinoma using multiplex quantitative analysis. *J. Transl. Med.* **18**, 306, https://doi.org/10.1186/s12967-020-02469-8

30 Liu, X. et al. (2019) PD-1(+) TIGIT(+) CD8(+) T cells are associated with pathogenesis and progression of patients with hepatitis B virus-related hepatocellular carcinoma. *Cancer Immunol. Immunother.* **68**, 2041–2054, https://doi.org/10.1007/s00262-019-02426-5

31 Wolf, M.J. et al. (2014) Metabolic activation of intrahepatic CD8+ T cells and NKT cells causes nonalcoholic steatohepatitis and liver cancer via cross-talk with hepatocytes. *Cancer Cell* **26**, 549–564, https://doi.org/10.1016/j.ccell.2014.09.003

32 Kalathil, S.G. et al. (2019) Augmentation of IFN-gamma+ CD8+ T cell responses correlates with survival of HCC patients on sorafenib therapy. *JCI Insight* **4**, e130116, https://doi.org/10.1172/jci.insight.130116

33 Takeda, K. et al. (2017) IFN-gamma is required for cytotoxic T cell-dependent cancer genome immunoediting. *Nat. Commun.* **8**, 14607, https://doi.org/10.1038/ncomms14607

34 Ye, L. et al. (2019) CD8+CXCR5+T cells infiltrating hepatocellular carcinomas are activated and predictive of a better prognosis. *Aging (Albany NY)* **11**, 8879–8891, https://doi.org/10.18632/aging.102308

35 Wu, Q. et al. (2019) Blocking triggering receptor expressed on myeloid cells-1-positive tumor-associated macrophages induced by hypoxia reverses immunosuppression and anti-programmed cell death ligand 1 resistance in liver cancer. *Hepatology* **70**, 198–214, https://doi.org/10.1002/hep.30593

36 Zheng, C. et al. (2017) Landscape of infiltrating T cells in liver cancer revealed by single-cell sequencing. *Cell* **169**, 1342e16–1356e16, https://doi.org/10.1016/j.cell.2017.05.035

37 Cui, N. et al. (2017) Biochemical and biological attributes of matrix metalloproteinases. *Prog. Mol. Biol. Transl. Sci.* **147**, 1–73, https://doi.org/10.1016/bs.pmbts.2017.02.005

38 Wang, G. et al. (2017) Loss of Barx1 promotes hepatocellular carcinoma metastasis through up-regulating MGAT5 and MMP9 expression and indicates poor prognosis. *Oncotarget* **8**, 71867–71880, https://doi.org/10.18632/oncotarget.18288

39 Liu, G. et al. (2020) M2 macrophages promote HCC cells invasion and migration via miR-149-5p/MMP9 signaling. *J. Cancer* **11**, 1277–1287, https://doi.org/10.7150/jca.35444

40 Sun, S.J. et al. (2018) MiR-5692a promotes the invasion and metastasis of hepatocellular carcinoma via MMP9. *Eur. Rev. Med. Pharmacol. Sci.* **22**, 4869–4878

41 Min, J. et al. (2018) IFITM3 promotes hepatocellular carcinoma invasion and metastasis by regulating MMP9 through p38/MAPK signaling. *FEBS Open Bio.* **8**, 1299–1311, https://doi.org/10.1002/2211-5463.12479
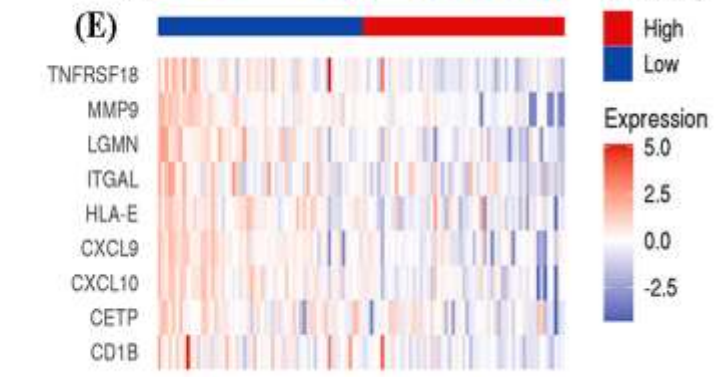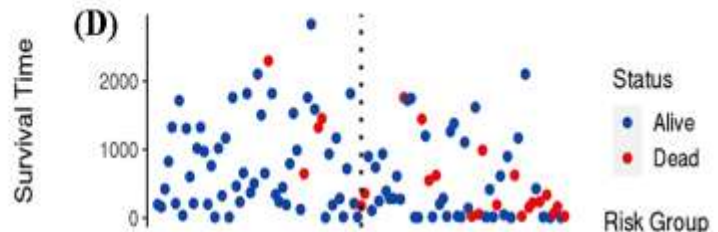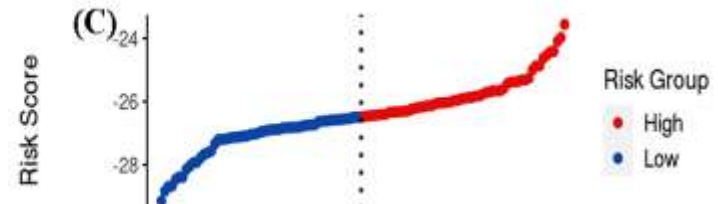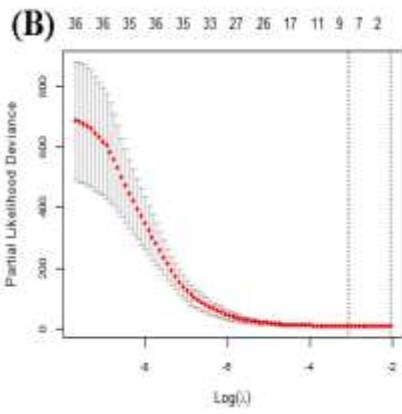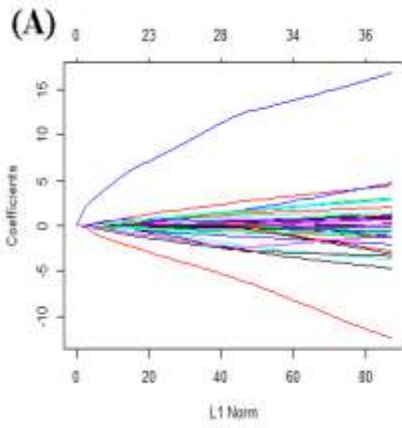
Table S1 Symbol and gene name correspondence list

Symbol	Gene name
CD1B	CD1b molecule
CETP	cholesteryl ester transfer protein, plasma
CXCL10	chemokine (C-X-C motif) ligand 10
CXCL9	chemokine (C-X-C motif) ligand 9
HLA-E	human leucocyte antigen, E
ITGAL	integrin alpha L
LGMN	legumain
MMP9	matrix metallopeptidase 9
TNFRSF18	TNF-receptor-superfamily-member 18
CD8A	CD8a molecule
CD8B	CD8b molecule
PD-1	programmed death 1
PD-L1	programmed death ligand 1
CART	chimeric antigen receptor T cells
CTLA4	cytotoxie Tlymphocyte associated antigen 4